

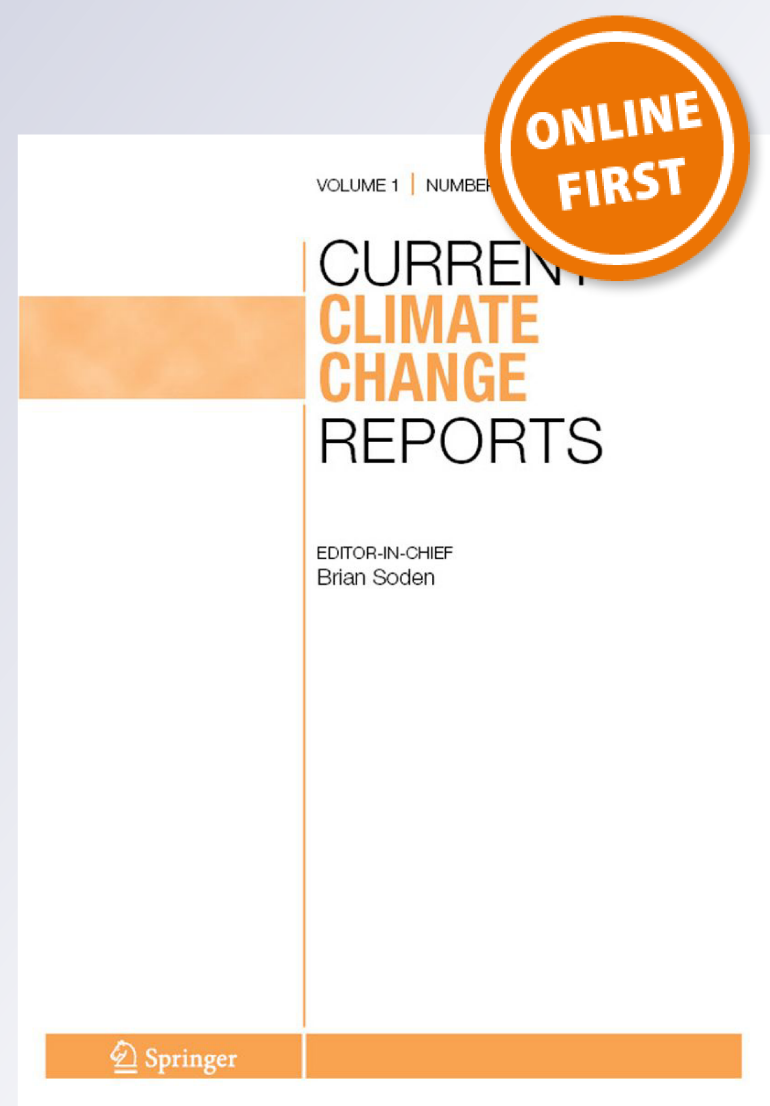
Climate Change and Drought: a Precipitation and Evaporation Perspective

Aiguo Dai, Tianbao Zhao & Jiao Chen

Current Climate Change Reports

e-ISSN 2198-6061

Curr Clim Change Rep
DOI 10.1007/s40641-018-0101-6



 Springer

Your article is protected by copyright and all rights are held exclusively by Springer International Publishing AG, part of Springer Nature. This e-offprint is for personal use only and shall not be self-archived in electronic repositories. If you wish to self-archive your article, please use the accepted manuscript version for posting on your own website. You may further deposit the accepted manuscript version in any repository, provided it is only made publicly available 12 months after official publication or later and provided acknowledgement is given to the original source of publication and a link is inserted to the published article on Springer's website. The link must be accompanied by the following text: "The final publication is available at link.springer.com".

Climate Change and Drought: a Precipitation and Evaporation Perspective

Aiguo Dai^{1,2} · Tianbao Zhao³ · Jiao Chen^{4,1}

© Springer International Publishing AG, part of Springer Nature 2018

Abstract

Many studies have shown that greenhouse gas (GHG)-induced global warming may lead to increased surface aridity and more droughts in the twenty-first century due to decreased precipitation in the subtropics and increased evaporative demand associated with higher vapor pressure deficit under warmer temperatures. Some recent studies argue that increased water use efficiency by plants under elevated CO₂ may reduce the evaporative demand and therefore mitigate the drying. Here we first discuss the model-projected changes in precipitation amount and frequency that affect the surface water balance and aridity and then the changes in actual and potential evapotranspiration under GHG-induced warming. The effects of the GHG-induced warming and changes in plants' physiology under elevated CO₂ on precipitation, soil moisture, and runoff are quantified and compared by analyzing different model experiments with and without the physiologic response. The surface drying effect of GHG-induced warming is found to dominate over the wetting effect of plants' physiology in response to increasing CO₂, leading to similar surface drying patterns in climate model simulations with or without the physiologic response in the twenty-first century. Part of the drying comes from increased dry spells (i.e., more dry days) and a flattening of the histograms of drought indices as GHGs increase, with the latter leading to widespread increases in hydrological drought even over areas with increasing mean runoff. Because of this, the change pattern of the mean cannot be used to represent drought changes. Consistent with the projected drying in the twenty-first century, recent analyses of model experiments suggest wetter land surfaces during the last glacial maximum, which implies that dusty air during cold glacial periods may have resulted from other factors, such as stronger winds and more dust sources, rather than drier land surfaces. Finally, the drying in the subtropics does not appear to be just a transient response to increased GHGs, as the warming and precipitation change patterns do not vary significantly over time in 500-year simulations with increased CO₂ contents by a fully coupled climate model.

Keywords Global warming · Climate projection · Drought · Precipitation · Evapotranspiration · Soil moisture · Runoff · Water use efficiency · Stomatal conductance · Last glacial maximum

Introduction and Outstanding Issues

This article is part of the Topical Collection on *Climate Change and Drought*

✉ Aiguo Dai
adai@albany.edu

¹ Department of Atmospheric and Environmental Sciences, University at Albany, SUNY, Albany, NY 12222, USA

² National Center for Atmospheric Research (NCAR), Boulder, CO, USA

³ Key Laboratory of Regional Climate-Environment Research for East Asia, Institute of Atmospheric Physics (IAP), Chinese Academy of Sciences (CAS), Beijing, China

⁴ School of Atmospheric Sciences, Nanjing University, Nanjing, China

Drought is a recurring extreme climate event over land characterized by below-normal precipitation and also often associated with warm temperatures over a period of months to years [2, 18, 65, 106]. Meteorological droughts are often defined using the lower tail of the probability density function (PDF) of normalized precipitation anomalies, while agricultural and hydrological droughts are measured by the lower tail of the PDFs of the indices related to soil moisture and streamflow, respectively [18, 58]. As such, drought changes (i.e., changes in drought frequency and area extent) may not be the same as those in the mean of the underlying metric (e.g., runoff or soil moisture), a point that is often overlooked.

Prolonged precipitation deficits often result in not only meteorological droughts but also agricultural and hydrological droughts. However, estimates of changes in historical [27] and model-projected future drought [9, 10, 15, 101, 102] may depend on which drought index one uses. Furthermore, up to now, historical changes in precipitation [1, 24, 27, 42] and drought [19, 20, 26, 27, 96–98, 108] are still dominated by internal climate variations such as those associated with the Inter-decadal Pacific Oscillation (IPO) and the Atlantic Multi-decadal Oscillation (AMO) [21, 33, 41, 52]; thus, comparisons between observed and model-simulated precipitation and drought changes need to be very careful [46, 50], as one might be comparing internal variability-induced multi-decadal changes with that induced by increasing greenhouse gases (GHGs). Because the two are likely to have very different spatial and temporal characteristics, such an inappropriate comparison may lead to misleading conclusions.

By definition, precipitation deficits are the primary cause of drought. What causes a prolonged precipitation deficit (and thus drought) over a certain region and time is often related to anomalous atmospheric circulation (often with high pressure) that suppresses the formation of clouds and precipitation [51, 69] or a shift in the rainbelt [95]. The reduction in clouds and precipitation leads to a drier surface, less evaporation, warmer temperatures, lower relative humidity, increased evaporative demand or potential evapotranspiration (PET), and thus further reduction in clouds and precipitation. These changes greatly enhance the drying initially triggered by the precipitation deficit, thereby worsening the drought condition [95]. Such a land-atmosphere feedback loop, which amplifies the drying caused by atmospheric circulation changes [4], can continue until a major change in weather patterns that brings substantial precipitation to the region to end the local feedback loop and the drought. A large number of studies [8, 16, 37, 40, 49, 53, 54, 56, 78, 83, 84, 87–89, 91, 95, 103] have shown that anomalous atmospheric circulation and prolonged precipitation deficits over many land regions, especially in North America, Africa, and Australia, can be caused by persistent sea surface temperature (SST) anomalies in the tropical and North Pacific and the North Atlantic, where SSTs often experience decadal to multi-decadal oscillations [60], although severe droughts over North America and other regions can occur without a clear SST forcing [51]. Recent attempts to predict seasonal droughts based on their links to SSTs have showed only limited skills [89].

Given the well-studied links between land precipitation and SSTs, and the dependence of regional precipitation response to greenhouse gas (GHG) forcing on SST change patterns [11, 100], one would expect that model-projected future changes in land precipitation and thus drought will depend on model-projected SST change patterns, which are found to be correlated with the spatial patterns of the temperature variance in current climate [22]. In particular, the predicted decrease in

subtropical precipitation (and thus drying in that region) in the twenty-first century [102] was linked to the meridional SST gradient [11]. Thus, current model projections of future precipitation and drought may be closely linked to their projected warming patterns, especially the meridional SST gradients in the low latitudes.

Many studies have only considered the impact of accumulative precipitation amount on drought, yet precipitation frequency (the fraction of time it precipitates) and intensity (the precipitation rate averaged over the precipitating time) also have significant effects on surface evaporation, runoff, soil moisture, and thus agricultural and hydrological droughts [76]. Climate models project large increases in precipitation intensity but decreases in frequency [28, 90, 94], which could potentially lead to more dry spells and floods [93]. Such an effect has not been included in most drought analyses, except those that make use of climate model output of soil moisture and runoff [85, 101, 102, 104], which already included this effect within the coupled climate models.

For changes in surface aridity (i.e., surface dryness or soil moisture content), agricultural and hydrological droughts under GHG-induced global warming, the increase in PET associated with rising air temperatures was first noticed by Dai et al. [26] and later found to be very important in many studies [34, 38, 80, 81, 101]. The primary cause for the ubiquitous PET increase is a large rise in surface vapor pressure deficit (VPD) in both recent observations and model projections [27, 36, 80] induced by rising air temperatures together with near constant surface relative humidity (RH) over land during recent periods [17, 43, 107] or slight decreases in the twenty-first century [12, 14]. Some recent studies (e.g., [6, 64, 92]) suggest that stomatal conductance reductions induced by elevated CO₂ levels [57, 62], increased water vapor demand [12, 70], and decreasing soil moisture [14, 101, 104] may reduce PET in future climate [7], yet these effects are often not considered in offline PET calculations.

However, as listed in Swann et al. [92], most of the CMIP5 models already either used the Ball–Berry ([3] (which is based on relative humidity and thus not a good measure of VPD) or the Leuning ([59] (which is based on VPD) stomatal conductance formulation to account for the effect of elevated CO₂ and changes in humidity on leaf stomatal conductance, although improvements are still needed, especially for accounting for the effects from decreasing soil moisture and increasing VPD (mainly for models using the Ball–Berry formulation) [7]. Thus, the stomatal effect of increased CO₂ has already been included in most of the CMIP5 model simulations while the effects of rising VPD and decreasing soil moisture are not fully considered. Analyses of the near-surface soil moisture directly from the CMIP5 models that already considered the stomatal effect of elevated CO₂ still suggest widespread drying in the twenty-first century [14, 101]. In fact, the drying indicated by near-surface soil moisture changes is more

severe than that implied by the offline calculated Palmer Drought Severity Index (PDSI; [19]) for 14 CMIP5 models [101]. This suggests that the surface drying effect from the GHG-induced warming dominates over any wetting effects [92] from plant physiological response to elevated CO₂ levels. A recent study [5] shows that the drying is less severe in subsurface soils, which is consistent with a drying caused by increased surface evaporative demand, as the surface drying signal takes decades to centuries to propagate downward into deeper layers. This may be good news for plants that have deep roots to access subsurface soil water. However, a large surface drying could still have major adverse impacts on crops, grasslands, forest fires, and heat waves. It could also reduce surface evaporation, enhance surface warming, and trigger a positive feedback loop that reduces land precipitation as described above [4].

Clearly, there exist large uncertainties in current estimates of future aridity and drought changes in the twenty-first century besides those associated with low [101, 102] and high [15] emission scenarios. Despite these uncertainties, the drying effect on land surface of a rising VPD associated with surface warming appears to dominate over secondary effects from plants' response to increasing CO₂ and changing climate conditions.

Precipitation Change and Its Impact on Future Drought

Regional and local precipitation is much more variable from year to year than temperature. This makes it much harder to predict future precipitation changes. For a given region, actual precipitation for a future time (e.g., the 2090s) will be a combination of the GHG-induced change and the internal-variability-induced anomalies at that location, and the latter could still dominate over the GHG-induced change even by the mid-late twenty-first century over certain regions [30]. Currently, we cannot predict, with a time lead of years to decades, future precipitation anomalies induced by internal variability, e.g., by ENSO [25] and the Interdecadal Pacific Oscillation (IPO) [21, 33, 42]; thus, the focus is often on the GHG-induced long-term changes, which can be best represented using the change in the multi-model ensemble mean (e.g., Fig. 12.10 of [14]). It should be emphasized that long-term precipitation changes derived from a single or a few model simulations (e.g., from a regional model downscaling forced by one or several global model simulations) may contain substantial contributions from realization-dependent internal variability that should not be interpreted as part of the response to the GHG forcing. Thus, extra care is needed in constructing and interpreting GHG-induced climate changes [29].

Under increasing GHGs in the twenty-first century, annual precipitation amount (Fig. 1a, b) is projected to increase over most of Eurasia, tropical Africa, and extratropical North America, but to decrease in the subtropical regions, including areas around the Mediterranean Sea, southwestern North America, southern Africa, most of Australia, and parts of South America. Large inter-model spread exists over many regions such as Australia and South and Central America, partly due to large internal variability over these regions (Fig. 1a, b; [14, 35, 102]). The broad patterns of precipitation response to future GHG forcing, including the large percentage increase (30–50% under a moderate scenario or 6–15% per 1 K global warming; [14]) over the northern high latitudes and the inter-tropical convergence zone (ITCZ) and the 5–25% decrease (or 2–8%/1 K) in subtropical precipitation (Fig. 1a, b), are robust among the current and the previous generations of climate models [14, 63, 102]. The increase in high-latitude precipitation is mainly due to increased water vapor content associated with large warming there that increases large-scale precipitation formation, while the increase in the ITCZ is due to increased moisture convergence during deep convection associated large increases in low-level specific humidity [13]. The decrease in subtropical precipitation largely results from the increased drying effect by the descending motion there due to increased vertical gradient of specific humidity in a warmer climate, as water vapor content increases more in the lower levels than in the upper troposphere [13]. The poleward expansion of the subsidence zone also contributes to the precipitation decrease around the current edges of the subtropical dry zone (Fig. 1a, b; [79]).

Clearly, the decrease in precipitation amount over the subtropical land will lead to drier conditions there. However, besides these amount changes, precipitation frequency (Fig. 1e), mainly of light-moderate precipitation events (Fig. 1f), is projected to decrease over most of the globe except the high latitudes and the Pacific ITCZ, while the opposite change patterns are predicted for the number of dry days (Fig. 1d) [28, 63, 90, 94]. On the other hand, heavy precipitation is projected to increase greatly by 30–80% over most of the globe except the subtropics (Fig. 1c, g; [90]), which could lead to slightly increased runoff ratios over many low-latitude land areas (Fig. 3d; [101]). These additional changes in precipitation characteristics likely have contributed to the much wider drying in surface soil moisture than the areas with decreasing precipitation (Fig. 2a, b), although the increased evaporative demand under warmer temperatures is likely to be the dominant cause of this widespread surface drying [101]. These projected precipitation changes could also lead to more flash floods [23, 47] and flash droughts [66, 67, 105]. However, these effects from the precipitation frequency and intensity changes are usually not included in offline drought calculations, including the calculated Palmer Drought Severity Index (PDSI) [15, 19, 20, 101, 102].

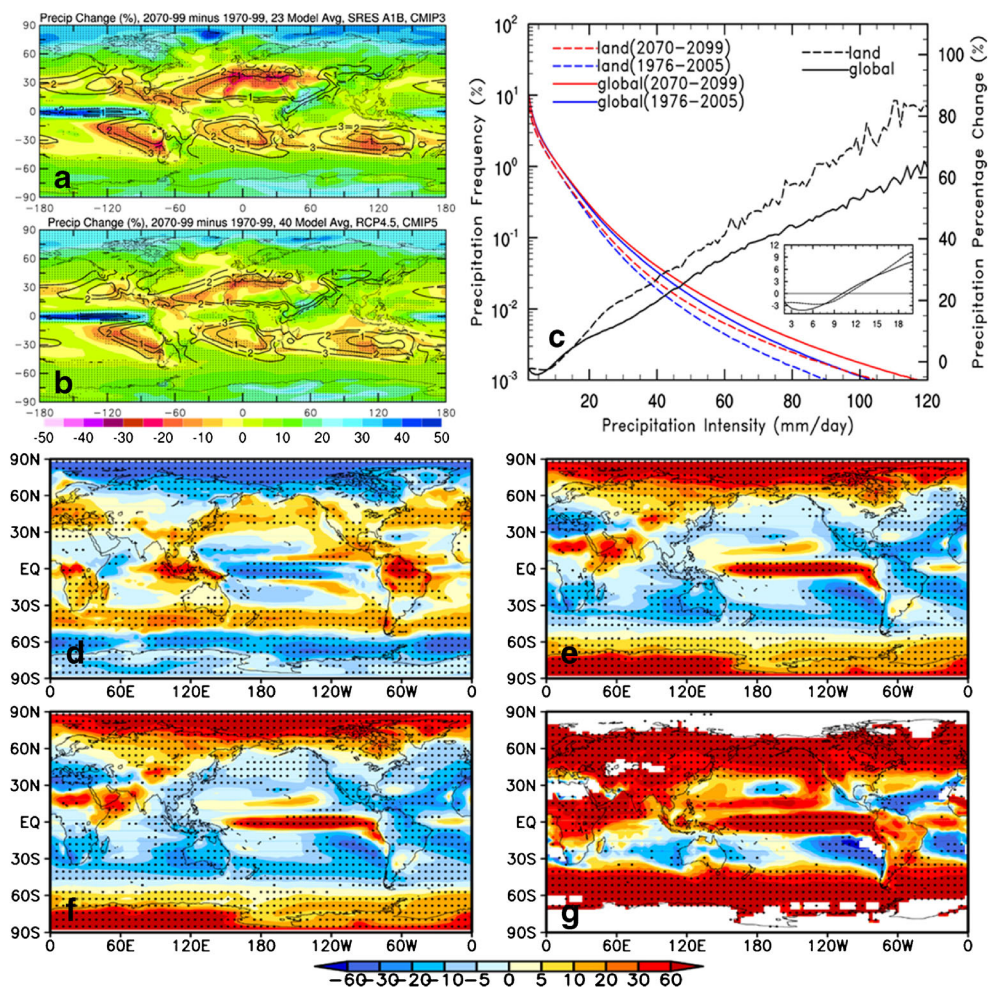


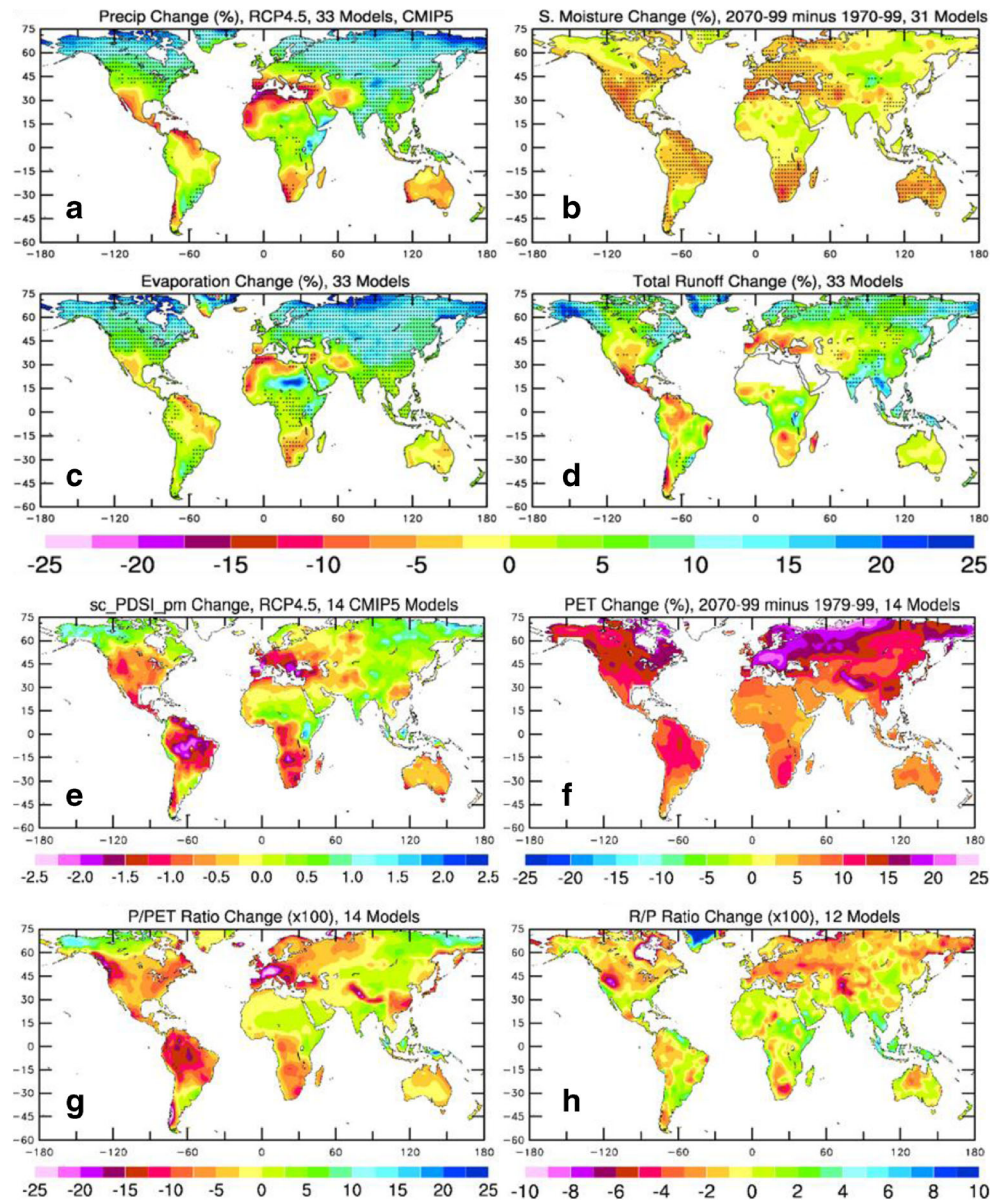
Fig. 1 Multi-model simulated precipitation changes. **a** Percentage change in annual precipitation amount from 1970–1999 to 2070–2099 simulated by 23 CMIP3 models under the moderate SRES A1B scenario. **b** Same as **a** but for 40 CMIP5 models under the low-moderate RCP4.5 scenario. The contours of 1, 2, and 3 mm/day for the 1970–1999 mean precipitation outline the current subtropical dry zone in the models. See <http://cmip-pcmdi.llnl.gov/> for a list of the CMIP models. (Modified from [102]). **c** Globally and land-averaged mean histograms of daily precipitation (for $P \geq 1$ mm/day, with a bin size of 1 mm/day) for a present (1976–2005, blue lines) and a future (2070–2099, red lines) 30-year period under the RCP8.5 scenario, with the histograms derived by combining all days together at each grid box first and then averaging the histograms

spatially for each model and then over 25 CMIP5 models. The percentage change of the frequency from the present to future periods is shown by the black lines (dashed for land and solid for global) on the right-hand y -axis. The small insert is a blowout for the percentage frequency change for the intensity below 20 mm/day. **d–g** The 25 CMIP5 model-averaged percentage change (in percentage of the 1976–2005 mean) from 1976–2005 to 2070–2099 under the RCP8.5 scenario in the frequency of **d** dry days (with $P < 0.1$ mm/day), **e** all types of precipitation (with $P \geq 1$ mm/day), **f** light-moderate precipitation ($1 \leq P < 20$ mm/day), and **g** heavy precipitation ($P \geq 20$ mm/day). Stippling indicates at least 80% of the models agree on the sign of change in **a**, **b** and **d–g**

Increased water vapor can largely explain the increases in heavy precipitation as it greatly increases the moisture convergence during a convective storm, while the decreases in light to moderate precipitation require other mechanisms [28]. One possible explanation is that on average surface evaporation may take a bit longer to replenish the moisture depleted by each future rainstorm, which depletes $\geq 7\%$ more moisture from the atmosphere per one-degree warming while surface evaporation increases by only about $2\%/\text{K}$, which constrains the global-mean precipitation amount change. This could lead to longer dry

spells and lower mean relative humidity (RH) and increased convective inhibition (CIN, i.e., the negative buoyancy) in a future warmer climate, all of which were confirmed by cloud-permitting simulations of future climates over the USA [28, 77]. The lower humidity and increased CIN could prevent some of the rain events from happening, especially for light-moderate precipitation events since they depend more on RH and atmospheric stability, thus leading to more dry spells and overall fewer rainy events at most mid-low latitude regions. More discussions on these issues can be found in Dai et al. [28].

Fig. 2 Multi-model mean long-term percentage changes from 1970–1999 to 2070–2099 (under a low-moderate RCP4.5 scenario) over land in annual **a** precipitation, **b** soil moisture content in the top 10 cm layer, **c** surface evapotranspiration, and **d** total runoff from 31 to 33 CMIP5 models. The stippling indicates at least 80% of the models agree on the sign of change. The change patterns are similar to those shown by Collins et al. [14]. (Adapted from [23]). **e–h** Same as **a–d** but for **e** self-calibrated PDSI with Penman–Monteith PET (**sc_PDSI_pm**), **f** PET calculated using the Penman–Monteith equation, **g** precipitation P vs. PET ratio ($\times 100$), and **h** runoff vs. P ratio or runoff ratio ($\times 100$) estimated using data from 14 CMIP5 models [12 for **h**]. For reference, a PDSI value below -1 is considered drought and below -3 is considered severe to extreme drought for current climate. (Adapted from [101])



Changes in PET and ET and Effects of Plant's Physiological Response

For agricultural and hydrological droughts, precipitation (P) changes are only one of the key factors. Another factor is the increasing atmospheric demand for moisture, as reflected by the ubiquitous increases in PET under rising temperatures (Fig. 2f; [34, 39, 80, 101, 102]). As recognized by Palmer [71], for agricultural drought, it is the PET, not the actual evapotranspiration (ET), that matters for the calculation of the PDSI [19, 71] and other [48, 99] drought indices. This is because it is the difference between the water supply (mainly through precipitation) and demand (measured by PET) that determines

the aridity or dryness over a region, while the actual ET is often limited by the availability of water and thus it is tightly coupled to precipitation over many land areas, so that P-ET would not change much over time. This close coupling between P and ET is reflected by their similar change patterns under rising GHGs (Fig. 2a, c; [14, 23, 63]). The ET change patterns are in sharp contrast to the ubiquitous increases in PET (Fig. 2f) over global land, which are induced primarily by increased VPD under rising surface air temperatures and relatively stable relative humidity [80, 101, 102]. The combined effect of the P and PET changes lead to widespread drying in near-surface soil moisture (Fig. 2c) as well as in offline calculated PDSI (Fig. 2e; [15, 18, 20, 101, 102]).

For hydrological drought [75], change in the lower tail of the probability density function (PDF) of total runoff [23] is a better measure, which also suggests increased drought frequency in the twenty-first century over many land areas (Fig. 3c), albeit with smaller magnitudes and slightly less widespread than those implied by near-surface soil moisture or PDSI (Fig. 3a, b; [101]). This is in sharp contrast to the rising total runoff over many of the mid-high latitude land areas and South and East Asia (Fig. 2d). A flattening of the PDFs for both the soil moisture and runoff contributes to the increased drought frequency, besides the effect of a reduction in the mean (only over the subtropics for runoff; Fig. 2d; [101]). It should be emphasized that drought events are determined by the left tail of the PDF of an aridity measure (e.g.,

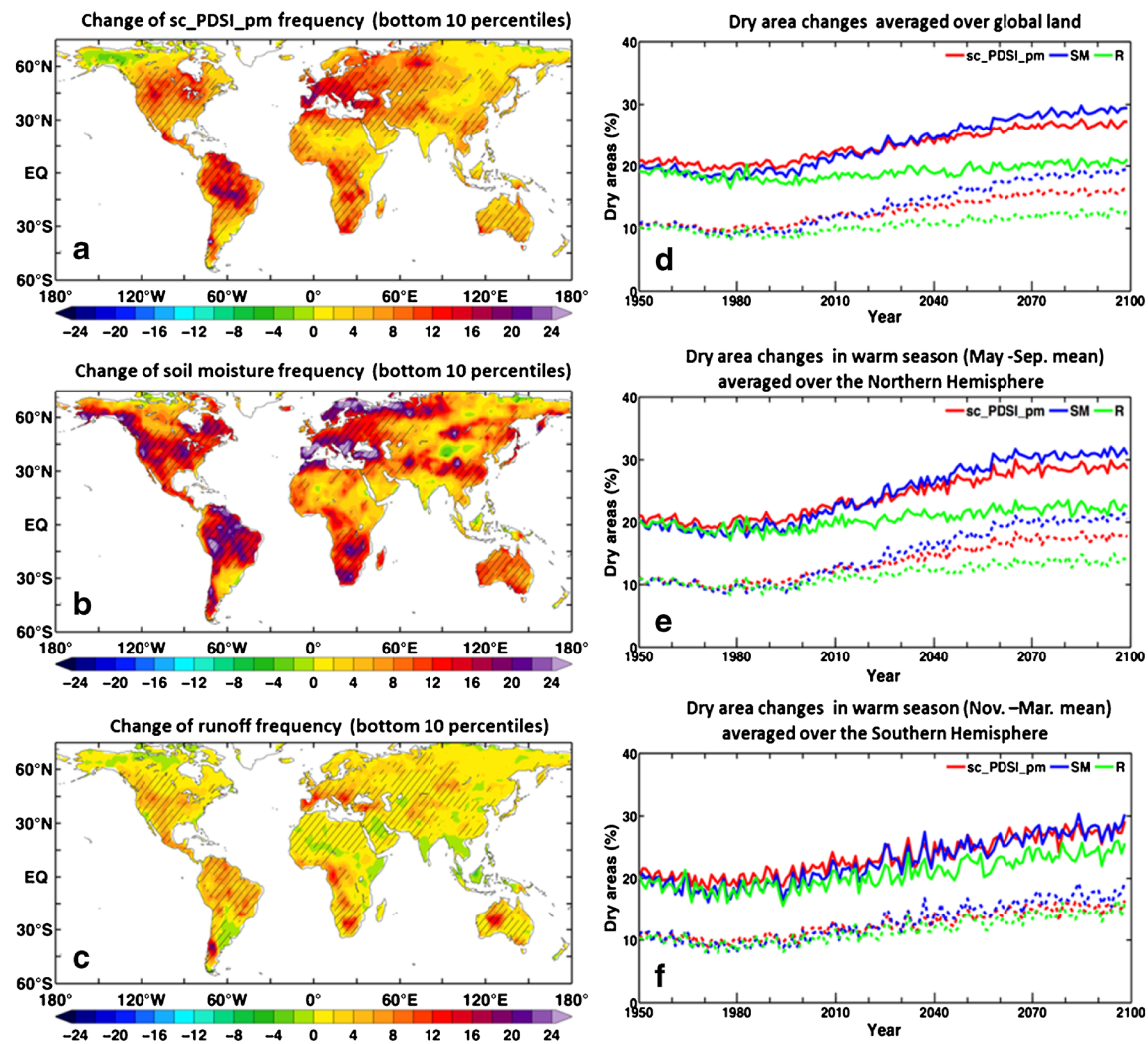


Fig. 3 Left: multi-model ensemble averaged changes of drought frequency (defined as the percentage of the time in drought conditions, not percentage changes) from 1970–1999 to 2070–2099 under the RCP 4.5 scenario, with drought events being defined locally as months below the 10th percentile of the 1970–1999 period based on monthly anomalies of **a** sc_PDSI_pm, **b** normalized soil moisture (SM) in the top 10 cm layer, and **c** normalized runoff (R) in individual model runs. The monthly anomalies of SM and R were normalized using the standard deviation over the 1970–1999 period. The stippling indicates at least

80% of the models agreeing on the sign of change. Right: multi-model ensemble mean time series of the drought areas (in percentage of the total land area between 60° S and 75° N) with the drought defined locally with monthly anomalies of sc_PDSI_pm (red), normalized monthly SM (blue) and R (green) below the 10th (dashed) or 20th (solid) percentile of the 1970–1999 period for **d** global land, **e** for warm season from May to September over Northern Hemisphere land, and **f** for warm season from November to March over Southern Hemisphere land. (Adapted from [101])

The increases in drought frequencies lead to upward trends in the percentage of global land areas under drought conditions during the twenty-first century for all types of drought based on PDSI, top 10 cm soil moisture, or total runoff, with the trend being largest based on the near-surface soil moisture and smallest based on the runoff (Fig. 3d–f). Annual P-ET is a good approximation of runoff as water storage changes are relatively small compared with the P or ET flux, and analyses

based on P-ET also showed reduced drying trends over land compared with PDSI-based estimates [92]. The drying in subsurface soil moisture is also smaller than near the surface by the late twenty-first century [5]. This is expected because surface signals (e.g., the diurnal cycle) penetrate downward with exponentially damped amplitudes (see Fig. 4.2 of [44]). Over decades to centuries, a land surface that loses water to the atmosphere associated with the surface drying will eventually lead to drier subsurface layers. However, current land surface models do not simulate well many subsurface processes (e.g., soil layer depth, vertical water exchange, groundwater, and permafrost layers). This makes the model-projected change in subsurface water content less reliable than that in the surface layer.

Recently, Milly and Dunne [64], Swann et al. [92], and Bonfils et al. [6] suggested that increased water use efficiency by plants under higher CO₂ levels through a reduction of stomatal conductance may significantly reduce the drying effect of rising temperatures and VPD, especially for offline calculated drought indices that do not take this effect into account. However, as stated above, the analyses using the precipitation, soil moisture, and runoff data directly from the CMIP5 models [101, 102] already included this effect in most of the models, and they still show widespread drying in near-surface soil moisture (Fig. 2b) and moderate increases in drought frequency based on runoff PDFs (Fig. 3c; [101]).

To further quantify this effect, we compared the changes in precipitation, top 10 cm soil moisture, and runoff in three experiments with 1% per year CO₂ increases from seven CMIP5 models (listed in Table S4 of [92]): (a) 1% per year CO₂ increase from pre-industrial level for both radiative processes and the carbon cycle (including photosynthesis); (b) same as (a) but the CO₂ increase is seen only in the carbon cycle, and it is fixed to the pre-industrial level for the radiative processes; and (c) same as (a) but the CO₂ increase is seen only by the radiative processes, and it is fixed in the carbon cycle. Similar to Swann et al. [92], we found that the radiative effect of increasing CO₂ dominates over plants' physiological response for precipitation, soil moisture, and runoff (Fig. 4), even though the latter does induce moderate wetting over Australia, Africa, South Asia, southern South America, and southwestern North America (Fig. 4e), which leads to slightly reduced drying in near-surface soil moisture over these regions in the case with both effects included (Fig. 4d) compared with the case with the radiative effect only (Fig. 4f). However, such an effect is overwhelmed by the large surface drying effect associated with rising air temperatures and VPD caused by the radiative effect of increasing CO₂, leading to similar surface drying patterns for the cases with (Fig. 4d) and without (Fig. 4f) the physiological effect. Thus, we conclude that the effect of plants' physiological response to increasing CO₂ is small compared with its radiative effect, leading to similar drying patterns in near-surface soil moisture in climate model simulations with or without the physiological response.

Issues in Estimating and Interpreting Historical Drought Changes

Estimating and interpreting recent drying trends over global land is challenging, not only because of the large internal variability in recent records of precipitation and other related fields, but also because large uncertainties exist in available datasets for precipitation, solar radiation, surface humidity, and wind speed that are needed to estimate PET and related drought indices [27, 96]. By synthesizing the changes in available records of precipitation, streamflow, and calculated PDSI, Dai and colleagues concluded that large drying trends have occurred since the 1950s over many low-latitude land areas, including most Africa, South and East Asia, southern Europe, eastern Australia, and many parts of the Americas [18–20, 26, 27]. However, a large part of these regional drying trends are likely due to the multi-decadal oscillations in Pacific and Atlantic SSTs, rather than GHG-induced global warming [27, 31, 54], and the drying trend is detectable only for the global mean, not at the regional level yet [20]. In contrast, Sheffield et al. [86] found much smaller drying trends over global land based on their calculated PDSI only. Further analyses [27, 96] suggest that the use of unreliable precipitation data after the mid-1990s and radiation data with large spurious trends by Sheffield et al. [86] likely contributed to their smaller drying trends. In any case, historical changes in land precipitation (and thus drought indices) are still dominated by internal climate variability [30, 32] and thus they should not be interpreted as and compared with model-simulated response to GHG forcing, as the two types of change have different spatial and temporal characteristics.

The Apparent Inconsistency with Paleoclimate Records

The model projected surface drying in the twenty-first century under increasing GHGs appears to be inconsistent with the notion that past cold climates are often characterized with dry or arid land, as reflected by sparse or treeless vegetation [45, 73] and a dusty atmosphere that led to elevated dust concentrations in polar ice core records [72] and increased dust deposition at many land sites [68]. However, the reduction in vegetation cover could be due to colder temperatures and reduced precipitation and CO₂ during glacial periods [74, 82], not necessarily due to increased aridity (i.e., drier soils). As stated by Muhs [68], the increased dust concentration may result from a number of factors, including increased source areas, greater aridity, less vegetation [74], lower soil moisture, stronger winds [61], a decreased intensity of the hydrologic cycle (thus less washout), and greater production of dust-sized particles from expanded ice sheets and glaciers. Analyses of numerical simulations of the last glacial maximum (LGM)

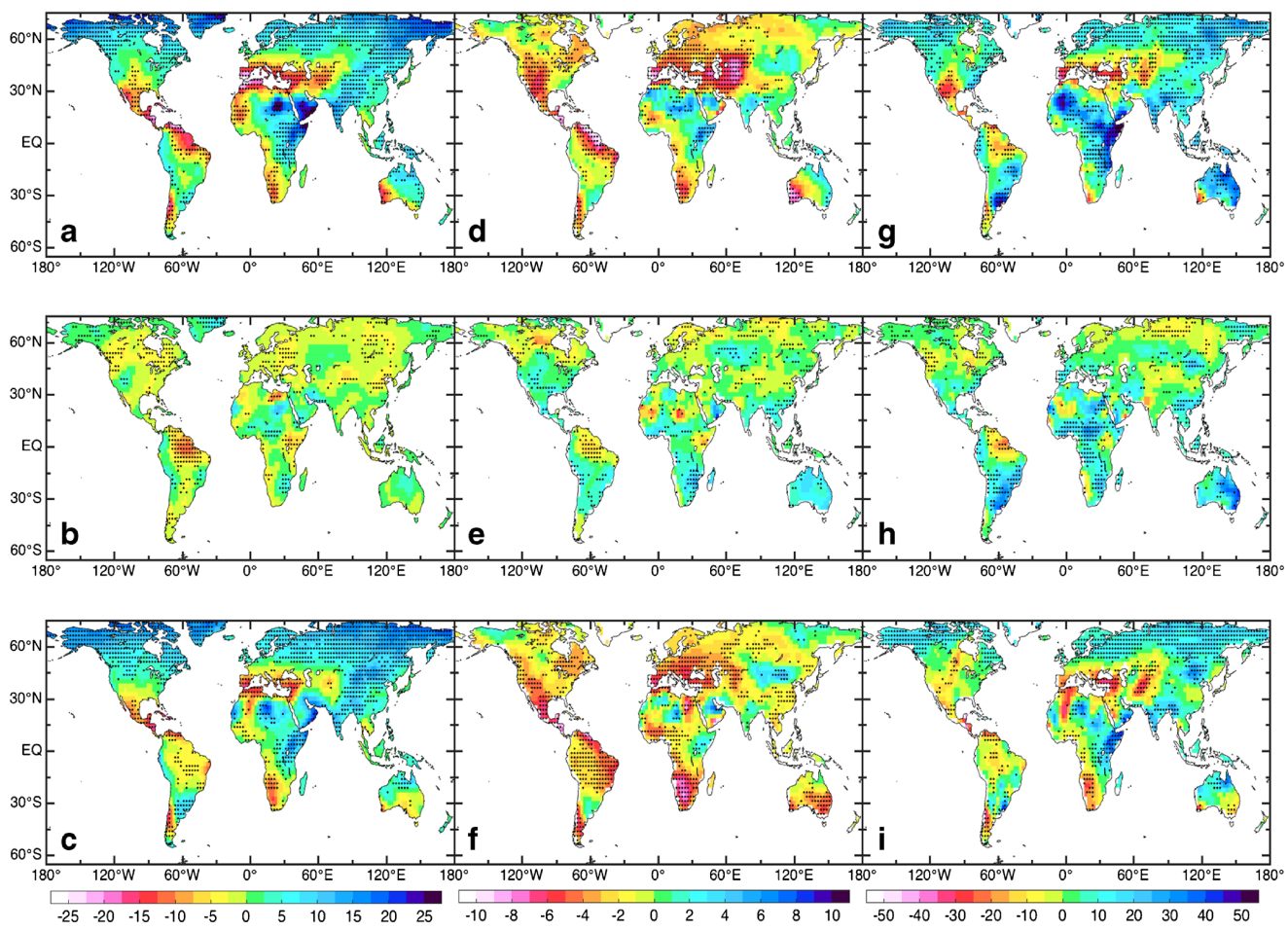


Fig. 4 Multi-model averaged percentage change in annual **a–c** precipitation, **d–f** top 10 cm soil moisture content, and **g–i** total runoff from year 61–80 (mean $\text{CO}_2 \approx 560 \text{ ppm}$) to year 121–140 (mean $\text{CO}_2 \approx 1031 \text{ ppm}$) from three different experiments: **a, d, g** with a 1% per year CO_2 increase seen by both radiative and physiological processes, **b, e, h** same as **a, d, g** but with atmospheric CO_2 fixed to the pre-industrial level in radiative processes, and **c, f, i** same as **a, d, g** but with fixed CO_2

in the carbon cycle (including photosynthesis). Dotted areas indicate at least five of the seven models agree on the sign of change. The following seven CMIP5 models had these simulations and were included in this analysis, and the plots are the ensemble average over them: bcc-csm1-1, CanESM2, CESM1-BGC, GFDL-ESM2M, HadGEM2-ES, IPSL-CM5A-LR, and NorESM1-ME

climate [82] suggest wetter top soils and less arid land by most common measures during the LGM than in the pre-industrial climate. Another modeling study [39] of the aridity changes from year 850 to 2080 showed that the P/PET ratio over global land decreases (i.e., becomes drier) during the warm periods but increases during the little ice age of 1550–1850 and other cold periods. Thus, increased aridity and a drier land surface may not be among the factors that contributed to the higher dust concentration in the previous cold climates. Therefore, one should not equate a dusty atmosphere with a dry land surface during glacial times, as pointed out previously (e.g., [61, 82]).

Another potential difference between the climate changes of the twenty-first century and those of past periods is that the paleoclimates are often averaged conditions over hundreds to millions of years, which may be best represented by the equilibrium climate response to increased GHGs, while the

twenty-first century climate is still a transient response to increasing GHGs. Some studies (e.g., [11]) suggest that the meridional SST gradient was different from today's climate during the warm early Pliocene Epoch about 3–5 million years ago, and this may be responsible for the wetter subtropics during the early Pliocene. This raises the question: Is the projected subtropical drying by the late twenty-first century only a transient response to increasing GHGs that may go away as the climate system approaches a new equilibrium? To address this question, we recently integrated a fully coupled climate model (namely the CESM1 from NCAR) for 500 years after an instantaneous doubling or quadrupling of the pre-industrial CO_2 level and then examined the change patterns in surface temperature and precipitation over time. The results [55] show that the surface warming patterns and the associated precipitation changes (including the subtropical drying) do not vary much over this 500-year period, over

which most of the expected equilibrium warming are already realized near the end of the simulation. This finding seems to suggest that the warming patterns and the associated precipitation changes of the twenty-first century are likely to be similar to those when the system reaches a new equilibrium. Thus, the difference between the transient and equilibrium change patterns is likely to be small and cannot explain the wetter subtropics during the early Pliocene.

Summary and Concluding Remarks

In this short review, we discussed some of the key issues in quantifying aridity and drought changes associated with GHG-induced global warming, with a focus on precipitation and evapotranspiration changes. Aridity of a region is traditionally measured by the annual P/PET ratio, which suggests increased aridity over most land areas by the end of twenty-first century (Fig. 3c). Normalized precipitation, soil moisture content, and runoff (or streamflow) are often used to quantify, respectively, meteorological, agricultural, and hydrological drought based on the lower tail of their PDFs (not their mean values). Annual precipitation amount are projected to increase over most land areas except the subtropical regions, where it decreases under rising GHGs which would lead to drier conditions there. Besides the amount changes, the frequency of light to moderate precipitation events is also projected to decrease over most of the globe except the high latitudes (Fig. 1c, f), and this leads to more dry spells (Fig. 1d) and thus likely also drier land conditions. Most of the precipitation amount increases outside the subtropics comes from increased heavy precipitation (due to increased water vapor), which may contribute to slight increases in runoff ratio over many low-latitude areas.

For surface aridity (or dryness), agricultural and hydrological droughts, changes in surface evaporative demand for moisture, often measured by PET, are also very important. Rising air temperatures with small changes in relative humidity lead to large increases in VPD, which in turn leads to ubiquitous increases in PET (Fig. 3b) over global land under increasing GHGs. Combined with increased dry days (Fig. 1d) and a flattening in the PDFs of soil moisture and runoff [101], the PET increases lead to large increases in agricultural drought events over most land as measured by the lower tail of the PDFs of the top-layer soil moisture and PDSI, while hydrological drought events increase at a more moderate rate (Fig. 3; [101]) as the mean runoff does not show widespread decreases as in surface soil moisture (Fig. 2).

Partly because of the flattening of the PDF for runoff, soil moisture, and PDSI [101], the change patterns in the mean of these and other (e.g., P-E) hydroclimate variables discussed in Milly and Dune [64], Swann et al. [92], Bonfils et al. [6], and other previous studies may not be representative of the change

patterns for drought frequency, which is determined by the lower tail of their PDFs. This basic difference has been overlooked, which may have contributed to some of the confusions in the literature regarding future drought changes. Also, the term “drying” is often used to describe a decreasing trend in mean precipitation, soil moisture, runoff, or P-E; thus, such a drying pattern only reflects the change in the mean, which may differ greatly from that for drought (which is a change in extremes), as shown by the mean runoff and hydrological drought case (Fig. 2d vs. Fig. 3c).

Plant’s physiological response to increased CO₂ levels, including the reduction in stomatal conductance, is likely to be only secondary compared with the dominant radiative effect of increasing CO₂. As a result, the surface drying patterns are similar in climate change simulations with or without the plant’s physiological response to elevated CO₂. This suggests that the effects of rising temperatures and VPD dominate over the effect of stomatal conductance reduction under increasing CO₂ for calculating PET and related drought indices. Furthermore, potential changes in aerodynamic and canopy resistances (e.g., due to elevated CO₂ levels) that affect evapotranspiration are already included in most CMIP5 models, which still show widespread drying in topsoil layers.

Recent modeling results [82] suggest that the land surface was indeed wetter during the last glacial maximum than the pre-industrial climate, which is consistent with the model-projected drying under increasing GHGs. Thus, the dusty atmosphere during cold glacial periods may not necessarily imply drier continents; instead, it could result from many other factors, such as stronger winds [61] and more dust sources as the land is covered with less vegetation [74, 82] during the cold climate [68].

Acknowledgments We acknowledge the CMIP5 modeling groups and NCAR CESM project, the Program for Climate Model Diagnosis and Intercomparison, and the WCRP’s Working Group on Coupled Modelling for their roles in making available the WCRP CMIP multi-model datasets. We thank Dr. Abby Swann of the University of Washington for sharing some of her downloaded CMIP5 model data that were used in Fig. 4.

Funding Information A. Dai acknowledges the funding support from the U.S. National Science Foundation (Grant #AGS-1353740 and #OISE-1743738), the U.S. Department of Energy’s Office of Science (Award No. DE-SC0012602), and the U.S. National Oceanic and Atmospheric Administration (Award No. NA15OAR4310086).

Compliance with Ethical Standards

Conflict of Interest On behalf of all authors, the corresponding author states that there is no conflict of interest.

Human and Animal Rights and Informed Consent This study does not involve human and animal rights in any way.

References

1. Adler RF, Gu G, Sapiano M, Wang J-J, Huffman GJ. Global precipitation: means, variations and trends during the satellite era (1979–2014). *Surv Geophys*. 2017;38:679–99. <https://doi.org/10.1007/s10712-017-9416-4>.
2. American Meteorological Society (AMS) (2013) Drought—an information statement. [<https://www.ametsoc.org/ams/index.cfm/about-ams/ams-statements/statements-of-the-ams-in-force/drought>].
3. Ball JT, Woodrow IE, Berry JA (1987) Progress in photosynthesis research, Biggins J (ed.), Martinus Nijhoff, Dordrecht, The Netherlands, pp. 221–224.
4. Berg A, et al. Land–atmosphere feedbacks amplify aridity increase over land under global warming. *Nat. Clim. Chang.* 2016;6(9):869–74. <https://doi.org/10.1038/nclimate3029>.
5. Berg A, Sheffield J, Milly P. Divergent surface and total soil moisture projections under global warming. *Geophys Res Lett.* 2017;44:236–44. <https://doi.org/10.1002/2016GL071921>.
6. Bonfils C, Anderson G, Santer BD, Phillips TJ, Taylor KE, Cuntz M, et al. Competing influences of anthropogenic warming, ENSO, and plant physiology on future terrestrial aridity. *J. Climate.* 2017;30:6883–904. <https://doi.org/10.1175/JCLI-D-17-0005.1>.
7. Bonan G, Williams M, Fisher R, Oleson K. Modeling stomatal conductance in the earth system: linking leaf water-use efficiency and water transport along the soil–plant–atmosphere continuum. *Geosci. Model Dev.* 2014;7:2193–222.
8. Burgman RJ, Jang Y. Simulated U.S. drought response to interannual and decadal Pacific SST variability. *J. Climate.* 2015;28: 4688–705.
9. Burke EJ. Understanding the sensitivity of different drought metrics to the drivers of drought under increased atmospheric CO₂. *J. Hydrometeor.* 2011;12:1378–94. <https://doi.org/10.1175/2011JHM1386.1>.
10. Burke EJ, Brown SJ. Evaluating uncertainties in the projection of future drought. *J. Hydrometeor.* 2008;9:292–9.
11. Burls NJ, Fedorov AV. Wetter subtropics in a warmer world: contrasting past and future hydrological cycles. *Proceed Nat Acad Sci.* 2017;28:12,888–93. <https://doi.org/10.1073/pnas.1703421114>.
12. Byrne MP, O’Gorman PA. Understanding decreases in land relative humidity with global warming: conceptual model and GCM simulations. *J Climate.* 2016;29:9045–61. <https://doi.org/10.1175/JCLI-D-16-0351.1>.
13. Chou C, Neelin JD, Chen C-A, Tu J-Y. Evaluating the “rich-get-richer” mechanism in tropical precipitation change under global warming. *J. Climate.* 2009;22:1982–2005. <https://doi.org/10.1175/2008JCLI2471.1>.
14. Collins M et al. (2013) Long-term climate change: projections, commitments and irreversibility. In: Climate change 2013: the physical science basis. Contribution of Working Group I to the Fifth Assessment Report of the Intergovernmental Panel on Climate Change [Stocker, T.F., D. Qin, G.-K. Plattner, M. Tignor, S.K. Allen, J. Boschung, A. Nauels, Y. Xia, V. Bex and P.M. Midgley (eds.)]. Cambridge University Press, Cambridge, United Kingdom and New York, NY, USA.
15. Cook BI, Smerdon JE, Seager R, Coats S. Global warming and 21st century drying. *Climate Dyn.* 2014;43:2607–27.
16. Cook BI, Cook ER, Smerdon JE, Seager R, Williams AP, Coats S, et al. North American megadroughts in the Common Era: reconstructions and simulations. *WIREs Clim Change.* 2016;7:411–32. <https://doi.org/10.1002/wcc.394>.
17. Dai A. Recent climatology, variability and trends in global surface humidity. *J. Climate.* 2006;19:3589–606.
18. Dai A. Drought under global warming: a review. *WIREs. Clim Change.* 2011a;2:45–65.
19. Dai A. Characteristics and trends in various forms of the Palmer Drought Severity Index during 1900–2008. *J Geophys Res.* 2011b;116:D12115.
20. Dai A. Increasing drought under global warming in observations and models. *Nature. Clim Change.* 2013a;3:52–8.
21. Dai A. (2013b) The influence of the inter-decadal Pacific Oscillation on U.S. precipitation during 1923–2010. *Climate Dynamics*, 41: 633–646. DOI <https://doi.org/10.1007/s00382-012-1446-5>.
22. Dai A (2016a) Future warming patterns linked to today’s climate variability. *Sci Rep.* 6: 19110, doi:<https://doi.org/10.1038/srep19110>.
23. Dai A (2016b) Historical and future changes in streamflow and continental runoff: a review. Chapter 2 of terrestrial water cycle and climate change: natural and human-induced impacts, *Geophysical Monograph 221*, edited by QiuHong Tang and Taikan Oki, AGU, John Wiley & Sons, pp. 17–37.
24. Dai A, Fung IY, Del Genio AD. Surface observed global land precipitation variations during 1900–1988. *J Clim.* 1997;10: 2943–62.
25. Dai A, Wigley TML. Global patterns of ENSO-induced precipitation. *Geophys Res Lett.* 2000;27:1283–6.
26. Dai A, Trenberth KE, Qian T. A global dataset of Palmer Drought Severity Index for 1870–2002: relationship with soil moisture and effects of surface warming. *J Hydrometeorol.* 2004;5:1117–30. <https://doi.org/10.1175/JHM-386.1>.
27. Dai A, Zhao T. Uncertainties in historical changes and future projections of drought. Part I: estimates of historical drought changes. *Climatic Change.* 2017;144:519–33. <https://doi.org/10.1007/s10584-016-1705-2>.
28. Dai, A., R.M. Rasmussen, C. Liu, K. Ikeda, and A.F. Prein (2017a) A new mechanism for warm-season precipitation response to global warming based on convection-permitting simulations. *Clim Dynamics*, DOI:<https://doi.org/10.1007/s00382-017-3787-6>.
29. Dai, A., R.M. Rasmussen, K. Ikeda, and C. Liu (2017b) A new approach to construct representative future forcing data for dynamic downscaling. *Clim Dynamics*, DOI: <https://doi.org/10.1007/s00382-017-3708-8>.
30. Dai, A., and C.E. Bloecker (2018) Impacts of internal variability on temperature and precipitation trends in large ensemble simulations by two climate models. *Clim Dynamics*, DOI: <https://doi.org/10.1007/s00382-018-4132-4>.
31. Delworth TL, Zeng F, Rosati A, Vecchi GA, Wittenberg AT. A link between the hiatus in global warming and North American drought. *J Climate.* 2015;28:3834–45.
32. Deser C, Phillips AS, Alexander MA, Smoliak BV. Projecting North American climate over the next 50 years: uncertainty due to internal variability. *J. Clim.* 2014;27:2271–96. <https://doi.org/10.1175/JCLI-D-13-00451.1>.
33. Dong B, Dai A. The influence of the inter-decadal Pacific Oscillation on temperature and precipitation over the globe. *Clim Dynamics.* 2015;45:2667–81. <https://doi.org/10.1007/s00382-015-2500-x>.
34. Feng S, Fu Q. Expansion of global dry lands under warming climate. *Atmos Chem Phys.* 2013;13:10081–10,094.
35. Feng S, Hu Q, Huang W, Ho CH, Li R, Tang Z. Projected climate regime shift under future global warming from multi-model, multi-scenario CMIP5 simulations. *Global Planet Change.* 2014;112:41–52. <https://doi.org/10.1016/j.gloplacha.2013.11.002>.
36. Ficklin DL, Novick KA. Historic and projected changes in vapor pressure deficit suggest a continental-scale drying of the United States atmosphere. *J Geophys Res Atmos.* 2017;122:2061–79. <https://doi.org/10.1002/2016JD025855>.

37. Findell KL, Delworth TL. Impact of common sea surface temperature anomalies on global drought and pluvial frequency. *J Clim*. 2010;23:485–503.

38. Fu Q, Feng S. Responses of terrestrial aridity to global warming. *J Geophys. Res. Atmos.* 2014;119:7863–75.

39. Fu Q, Lin L, Huang J, Feng S, Gettelman A. Changes in terrestrial aridity for the period 850–2080 from the Community Earth System Model. *J. Geop hys. Res. Atmos.* 2016;121:2857–73. <https://doi.org/10.1002/2015JD024075>.

40. Giannini A, Saravanan R, Chang P. Oceanic forcing of Sahel rainfall on interannual to interdecadal time scales. *Science*. 2003;302:1027–30.

41. Gu G, Adler RF. Interdecadal variability/long-term changes in global precipitation patterns during the past three decades: global warming and/or Pacific decadal variability? *Clim Dyn*. 2013;40: 3009–22. <https://doi.org/10.1007/s00382-012-1443-8>.

42. Gu G, Adler RF. Spatial patterns of global precipitation change and variability during 1901–2010. *J Clim*. 2015;28:4431–53. <https://doi.org/10.1175/JCLI-D-14-00201.1>.

43. Hartmann DL et al. (2013) Observations: atmosphere and surface. In: Climate change 2013: the physical science basis. Contribution of Working Group I to the Fifth Assessment Report of the Intergovernmental Panel on Climate Change [Stocker, T.F., D. Qin, G.-K. Plattner, M. Tignor, S.K. Allen, J. Boschung, A. Nauels, Y. Xia, V. Bex and P.M. Midgley (eds.)]. Cambridge University Press, Cambridge, United Kingdom and New York, NY, USA.

44. Hartmann DL. Global physical climatology. 2nd ed. Amsterdam: Elsevier; 2016. p. 485.

45. Hegerl, G. C. et al. 2007: Understanding and attributing climate change. Climate change 2007: the physical science basis, S. Solomon et al., Eds., Cambridge University Press, 663–745.

46. Hegerl GC, et al. Challenges in quantifying changes in the global water cycle. *Bull Am Met Soc*. 2015;96:1097–115. <https://doi.org/10.1175/BAMS-D-13-00212.1>.

47. Hirabayashi Y, Mahendran R, Koirala S, Konoshima L, Yamazaki D, Watanabe S, et al. Global flood risk under climate change. *Nat Clim Change*. 2013;3:816–21. <https://doi.org/10.1038/nclimate1911>.

48. Hobbins M, Wood A, McEvoy D, Huntington J, Morton C, Anderson M, Hain C (2016). The evaporative demand drought index. Part I: linking drought evolution to variations in evaporative demand. *J Hydrometeorol*, 17(6), 1745–1761. doi: <https://doi.org/10.1175/JHM-D-15-0121.1>

49. Hoerling M, Hurrell J, Eischeid J, Phillips A. Detection and attribution of twentieth-century northern and southern African rainfall change. *J. Climate*. 2006;19:3989–4008. <https://doi.org/10.1175/JCLI3842.1>.

50. Hoerling MP, Eischeid J, Perlitz J. Regional precipitation trends: distinguishing natural variability from anthropogenic forcing. *J. Climate*. 2010;23:2131–45. <https://doi.org/10.1175/2009JCLI3420.1>.

51. Hoerling MP, Eischeid J, Kumar A, Leung R, Mariotti A, Mo K, et al. Causes and predictability of the 2012 Great Plains drought. *Bull Amer Meteor Soc*. 2014;95:269–82.

52. Hu Q, Feng S. AMO- and ENSO-driven summertime circulation and precipitation variations in North America. *J Climate*. 2012;25: 6477–95. <https://doi.org/10.1175/JCLI-D-11-00520.1>.

53. Hu Q, Veres MC. Atmospheric responses to North Atlantic SST anomalies in idealized experiments. Part II: North Am Precipitation *J Climate*. 2016;29(2):659–71.

54. Huang J, Y. Li, C. Fu, F. Chen, Q. Fu, A. Dai, M. Shinoda, Z. Ma, W. Guo, Z. Li, L. Zhang, Y. Liu, H. Yu, Y. He, Y. Xie, X. Guan, M. Ji, L. Lin, S. Wang, H. Yan, and G. Wang (2017) Dryland climate change: recent progress and challenges. *Rev Geophys* 55: 719–778.

55. Huang, D., A. Dai, et al. (2018) Are the transient and equilibrium climate change patterns different in response to increased CO₂? To be submitted to *Climate Dynamics*.

56. Kam J, Sheffield J, Wood EF. Changes in drought risk over the contiguous United States (1901–2012): the influence of the Pacific and Atlantic Oceans. *Geophys Res Lett*. 2014;41:5897–903.

57. Katul G, Manzoni S, Palmroth S, Oren R. A stomatal optimization theory to describe the effects of atmospheric CO₂ on leaf photosynthesis and transpiration. *Ann Botany*. 2010;105:431–42.

58. Keyantash J, Dracup JA. The quantification of drought: an evaluation of drought indices. *Bull Am Met Soc*. 2002;83:1167–80.

59. Leuning R. A critical appraisal of a combined stomatal-photosynthesis model for C3 plants. *Plant Cell Environ*. 1995;18(4):339–55.

60. Liu ZY. Dynamics of interdecadal climate variability: a historical perspective. *J Clim*. 2012;25:1963–95.

61. McGee D, Broecker WS, Winckler G. Gustiness: the driver of glacial dustiness? *Quat Sci Rev*. 2010;29:2340–50. <https://doi.org/10.1016/j.quascirev.2010.06.009>.

62. Medlyn BE, et al. Reconciling the optimal and empirical approaches to modelling stomatal conductance. *Glob Change Biol*. 2011;21:2134–2144(2011):17.

63. Meehl, G.A., T.F. Stocker, W.D. Collins, P. Friedlingstein, A.T. Gaye, J.M. Gregory, A. Kitoh, R. Knutti, J.M. Murphy, A. Noda, S.C.B. Raper, I.G. Watterson, A.J. Weaver and Z.-C. Zhao (2007): Global climate projections. In: Climate change 2007: the physical science basis. Contribution of Working Group I to the Fourth Assessment Report of the Intergovernmental Panel on Climate Change [Solomon, S., D. Qin, M. Manning, Z. Chen, M. Marquis, K.B. Averyt, M. Tignor and H.L. Miller (eds.)]. Cambridge University Press, Cambridge, United Kingdom and New York, NY, USA.

64. Milly PCD, Dunne KA. Potential evapotranspiration and continental drying. *Nat Clim Change*. 2016;6:946–9. <https://doi.org/10.1038/NCLIMATE3046>.

65. Mishra AK, Singh VP. A review of drought concepts. *J Hydrol*. 2010;391:202–16. <https://doi.org/10.1016/j.jhydrol.2010.07.012>.

66. Mo KC, Lettenmaier DP. Heat wave flash droughts in decline. *Geophys Res Lett*. 2015;42:2823–9. <https://doi.org/10.1002/2015GL064018>.

67. Mo KC, Lettenmaier DP. Precipitation deficit flash droughts over the United States. *J Hydrometeorol*. 2016;17:1169–84.

68. Muhs DR. The geologic records of dust in the Quaternary. *Aeolian Res*. 2013;9:3–48. <https://doi.org/10.1016/j.aeolia.2012.08.001>.

69. Namias J. Some causes of United States drought. *J Clim Appl Meteor*. 1983;22:30–9.

70. Novick K, et al. The increasing importance of atmospheric demand for ecosystem water and carbon fluxes. *Nat Clim Chang*. 2016;6(11):1023–7. <https://doi.org/10.1038/nclimate3114>.

71. Palmer WC (1965) *Meteorological drought*. Research Paper No. 45, US Dept. of Commerce, pp. 58. [Available from <http://www.ncdc.noaa.gov/oa/climate/research/drought/palmer.pdf>].

72. Petit JR, et al. Climate and atmospheric history of the past 420, 000 years from the Vostok ice core, Antarctica. *Nature*. 1999;399: 429–36. <https://doi.org/10.1038/20859>.

73. Prentice IC, et al. Mid-Holocene and glacial-maximum vegetation geography of the northern continents and Africa. *J. Biogeogr*. 2000;27:507–19. <https://doi.org/10.1046/j.1365-2699.2000.00425.x>.

74. Prentice IC, Harrison SP, Bartlein PJ. Global vegetation and terrestrial carbon cycle changes after the last ice age. *New Phytol*. 2011;189:988–98. <https://doi.org/10.1111/j.1469-8137.2010.03620.x>.

75. Prudhomme C, et al. Hydrological droughts in the 21st century, hotspots and uncertainties from a global multimodel ensemble experiment. *Proc Natl Acad Sci USA*. 2014;111(9):3262–7.

76. Qian T, Dai A, Trenberth KE, Oleson KW. Simulation of global land surface conditions from 1948–2004 Part I: forcing data and evaluation. *J Hydrometeorol*. 2006;7:953–75.

77. Rasmussen K L, Prein A F, Rasmussen R M, Ikeda K, and Liu C (2017) Changes in the convective population and thermodynamic environments in convection-permitting regional climate simulations over the United States. *Climate Dynamics*, doi: <https://doi.org/10.1007/s00382-017-4000-7>.

78. Routson CC, Woodhouse CA, Overpeck JT, Betancourt JL, McKay NP. Teleconnected ocean forcing of Western North American droughts and pluvials during the last millennium. *Quaternary Science Reviews*. 2016;146:238–50.

79. Scheff J, Frierson DMW. Robust future precipitation declines in CMIP5 largely reflect the poleward expansion of model subtropical dry zones. *Geophys. Res. Lett.* 2012;39:L18704. <https://doi.org/10.1029/2012GL052910>.

80. Scheff J, Frierson DMW. Scaling potential evapotranspiration with greenhouse warming. *J Clim.* 2014;27:1539–58. <https://doi.org/10.1175/JCLI-D-13-00233.1>.

81. Scheff J, Frierson DMW. Terrestrial aridity and its response to greenhouse warming across CMIP5 climate models. *J Clim.* 2015;28:5583–600.

82. Scheff J, Seager R, Liu H, Coats S. Are glacials dry? Consequences for paleoclimatology and for greenhouse warming. *J. Climate.* 2017;30:6593–609. <https://doi.org/10.1175/JCLI-D-16-0854.1>.

83. Schubert SD, Gutzler D, Wang HL, Dai A, Delworth T, et al. A US CLIVAR project to assess and compare the responses of global climate models to drought-related SST forcing patterns: overview and results. *J Clim.* 2009;22:5251–72.

84. Schubert SD, et al. Global meteorological drought: a synthesis of current understanding with a focus on SST drivers of precipitation deficits. *J Clim.* 2016;29:3989–4019.

85. Sheffield J, Wood EF. Projected changes in drought occurrence under future global warming from multi-model, multi-scenario, IPCC AR4 simulations. *Clim Dyn.* 2008;31:79–105.

86. Sheffield J, Wood EF, Roderick ML. Little change in global drought over the past 60 years. *Nature.* 2012;491(7424):435–8.

87. Seager R, Kushnir Y, Herweijer C, Naik N, Velez J. Modeling of tropical forcing of persistent droughts and pluvials over western North America: 1856–2000. *J Clim.* 2005;18:4068–91.

88. Seager R, Hoerling M. Atmosphere and ocean origins of North American droughts. *J Clim.* 2014;27(12):4581–606.

89. Seager R, Ting M. Decadal drought variability over North America: mechanisms and predictability. *Curr Clim Change Rep.* 2017;3:141–9.

90. Sun Y, Solomon S, Dai A, Portmann R. How often will it rain? *J Climate.* 2007;20:4801–18.

91. Sun Q, Miao C, AghaKouchak A, Duan Q. Century-scale causal relationships between global dry/wet conditions and the state of the Pacific and Atlantic Oceans. *Geophys Res Lett.* 2016;43(12): 6528–37. <https://doi.org/10.1002/2016GL069628>.

92. Swann ALS, Hoffman FM, Koven CD, Randerson JT. Plant responses to increasing CO₂ reduce estimates of climate impacts on drought severity. *Proc Natl Acad Sci USA.* 2016;113:10019–10, 024. <https://doi.org/10.1073/pnas.1604581113>.

93. Trenberth KE. Changes in precipitation with climate change. *Clime Res.* 2011;47:123–38. <https://doi.org/10.3354/cr00953>.

94. Trenberth, K. E., A. Dai, R. M. Rasmussen, and D. B. Parsons (2003) The changing character of precipitation. *Bull Amer Meteorol Soc.*, 84, 1205–1217.

95. Trenberth KE, Branstator GW, Arkin PA. Origins of the 1988 North American drought. *Science.* 1988;242:1640–6.

96. Trenberth KE, Dai A, van der Schrier G, Jones PD, Barichivich J, Briffa KR, et al. Global warming and changes in drought. *Nature Climate Change.* 2014;4:17–22.

97. van der Schrier G, Jones PD, Briffa KR. The sensitivity of the PDSI to the Thornthwaite and Penman-Monteith parameterizations for potential evapotranspiration. *J Geophys Res Atmos.* 2011;116:D03106. <https://doi.org/10.1029/2010JD015001>.

98. van der Schrier G, Barichivich J, Briffa KR, Jones PD. A scPDSI-based global data set of dry and wet spells for 1901–2009. *J Geophys Res Atmos.* 2013;118:4025–48. <https://doi.org/10.1002/2012JD019355>.

99. Vicente-Serrano SM, Beguería S, López-Moreno JI. A multi-scalar drought index sensitive to global warming: the Standardized Precipitation Evapotranspiration Index—SPEI. *J Clim.* 2010;23:1696–718.

100. Xie S, Deser C, Vecchi GA, Ma J, Teng H, Wittenberg AT. Global warming pattern formation: sea surface temperature and rainfall. *J Clim.* 2010;23:966–86. <https://doi.org/10.1175/2009JCLI3329.1>.

101. Zhao T, Dai A. The magnitude and causes of global drought changes in the 21st century under a low–low-moderate emissions scenario. *J Clim.* 2015;28:4490–512.

102. Zhao T, Dai A. Uncertainties in historical changes and future projections of drought. Part II: model-simulated historical and future drought changes. *Clim Change.* 2017;144:535–48. <https://doi.org/10.1007/s10584-016-1742-x>.

103. Zhao S, Deng Y, and Black RX (2017) Observed and simulated spring and summer dryness in the United States: the impact of the Pacific Sea surface temperature and beyond. *J Geophys Res.* 122. doi: <https://doi.org/10.1002/2017JD027279>

104. Wang GL. Agricultural drought in a future climate: results from 15 global climate models participating in the IPCC 4th assessment. *Clim Dyn.* 2005;25:739–53.

105. Wang L, Yuan X, Xie Z, Wu P, Li Y. Increasing flash droughts over China during the recent global warming hiatus. *Sci Rep.* 2016;6:30571. <https://doi.org/10.1038/srep30571>.

106. Wilhite DA (2000) Drought as a natural hazard: concepts and definitions. In *Droughts: a global assessment*, Wilhite DA (Ed.), Routledge, pp.3–18.

107. Wilhite KM, Jones PD, Gillett NP, Thorne PW. Recent changes in surface humidity: development of the HadCRUH dataset. *J Clim.* 2008;21:5364–83.

108. Williams AP, Seager R, Abatzoglou JT, Cook BI, Smerdon JE, Cook ER. Contribution of anthropogenic warming to California drought during 2012–2014. *Geophys Res Lett.* 2015;42(16): 6819–28. <https://doi.org/10.1002/2015GL064924>.